Determination of plateau widths and energy gaps in the fractional quantum Hall effect by multi-particle correlations

Jongbae Hong
Research Institute of Basic Sciences, Incheon National University, Yeonsu-gu, Incheon 22012, Korea
(Dated: June 11, 2019)

The fractional quantum Hall effect (FQHE) has been considered as a puzzling quantum many-body phenomenon that has yet to be fully explained. The experimentally measured Hall resistivity curve must be clarified based on quasiparticle energy gaps, and therefore, revealing the relation between plateau widths and energy gaps is key to fully understand the electron transport that causes the FQHE. Here, we report that a quasiparticle of spin unity comprising an electron and its image replacing the confining potential of an incompressible strip appropriately describes the dynamics of electrons moving through the narrow strip under high magnetic field, and also that correlated quasiparticles formed by many-body interaction have higher integral spins and play a crucial role. The Zeeman effect for individual quasiparticles of spin unity splits a degenerated Landau level into three sublevels, which produces plateaus of filling factor with denominator three, and each sublevel splits again into five sublevels due to two correlated quasiparticles with total spin two, which produces plateaus of filling factors with denominator five. This level splitting continues with higher-order quasiparticle correlation. With such a scheme, we explicitly show that plateau widths and energy gaps are connected via the degrees of multi-particle correlation and reproduce experimental Hall resistivity and energy gaps, Only the lowest Landau level is studied, where plateaus of even-denominator filling factors do not appear.

PACS numbers:

Two-dimensional electron systems often exhibit marvelous phenomena (1–3), with one being the fractional quantum Hall effect (FQHE) (2). It is well known that in a clean two-dimensional system at low temperature under a strong perpendicular magnetic field, many plateaus are observed at various fractional filling ν in Hall resistivity. Most fractions have odd denominators except for special cases. Even though the Laughlin wavefunction (4) provides the basic idea behind the effect and the composite fermion theory (5, 6) picks up most of the observed plateaus, these cannot reproduce the experimental Hall resistivity curve (7). The reason may be attributable to the nature of equilibrium theories based on magnetic flux, which is not defined for cycloidal motion produced under Hall bias. Since Hall resistivity is a phenomenon of current flow under Hall bias, essential pieces of information, i.e., where and how the Hall current flows, may be crucial to explain the behavior of Hall resistivity.

Halperin (8) first proposed electron flow in the edge of a Hall bar due to Landau level (LL) bending by the confining potential. However, the previous studies (9, 10) on edge current were unsuccessful in explaining the FQHE. Some years ago, experimentalists (11–13) observed incompressible strips along the edge of a Hall bar in an integral quantum Hall system, through which Hall current flows. Theoretical studies (14, 15) have already predicted the existence of such incompressible strips in the edge region. We sketch compressible and incompressible strips distinguished by electron density profile in Fig. 1(a). Recently, Hall potential was measured in a fractional quantum Hall (FQH) system around $\nu = 2/3$ using a scanning probing microscope (16); the result clearly shows that Hall current flows in both edge and bulk regions depending on the strength of the magnetic field. A related schematic is sketched in the inset of Fig. 1(a) to which we added incompressible strips. Notable points are i) the width covered by the Hall current, about 5 μm, is two orders of magnitude wider than the magnetic length scale $(\hbar/eB)^{1/2}$, and ii) Hall current flows symmetrically on the left and right sides. The first feature can be explained by allocating multiple incompressible strips, but the second feature requires information on how the Hall current actually flows through the incompressible strip.

It is well known that electrons follow a cycloidal motion when they move forward under a high magnetic field. However, in a narrow confined region such as incompressible strip, the motion changes to a skipping form at the edge and a deformed cycloidal form away from the edge, as sketched in Fig. 1(b). Then, the direction of motion at both edges must be opposite, and the deformed cycloidal motion will be slower than the skipping motion because the former has a longer path. Different directions and speeds in an incompressible strip declare the existence of a well-type potential $V_C(y)$ (red line) in Fig. 1(b) because the slope of potential reflects the group velocity of a carrier. We show in Fig. 1(c) that this well-type potential naturally produces a left–right symmetric Hall current under Hall bias. This explains the second feature of Hall current. The well-type potential has not been explicitly shown by calculations using a simplified model (14) or the Thomas–Fermi approximation (15). More sophisticated calculations are likely needed.

Now, we study electron motion in a well-type confining potential. To describe it more effectively, we introduce an image charge $-q$ with the same spin, as depicted in Fig. 1(d), thereby securing that the electron wavefunction will not leak out of the incompressible strip due to the Pauli principle as well as eliminating the confining

potential. The amount of image charge $-q$ could vary in position to fit the confining potential, but we neglect the Coulomb effect between the electron and image charge in obtaining the splitting in the lowest Landau level (LLL) shown in Fig. 2. The strong magnetic field produces a bound motion, as illustrated in Fig. 1(e), and yields a quasiparticle of spin-state $|\chi_{\downarrow\downarrow}\rangle$ indicating a total spin of $S = 1$. Thus, the basic quasiparticles formed in Hall current flow are composite bosons of spin unity. Next, we introduce many-body correlations among electrons induced by inter-electron interactions in a two-dimensional layer, which cause the correlated multi-quasiparticle motion sketched in Fig. 1(f) for correlated two quasiparticles whose spin-state is given by $|\chi_{\downarrow\downarrow\downarrow\downarrow}\rangle$ with total spin $S = 2$. One can easily imagine correlated three-quasiparticle motion with $S = 3$ and more multi-quasiparticle motions in the same manner.

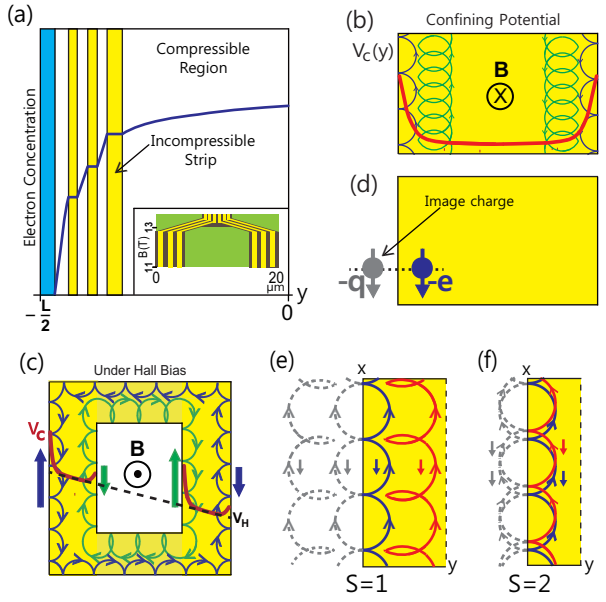

FIG. 1: Electron dynamics in a FQH system. (a) Electron concentration in the left half of a Hall bar of width L is presented by the dark blue line. Three incompressible strips (yellow) having constant electron concentration, compressible regions (white), and a depletion region (blue) are shown. The inset depicts the schematic of an incompressible strip in the region of Hall current (brown) (16). (b) Electron motions and confining potential in the incompressible strip shown in (a). The skipping motion (blue) is faster than the deformed cycloidal one (green), which is consistent with the slope of the potential (red). (c) Electron motions in a full incompressible strip under Hall bias V_H. The big arrows show that V_H induces a left–right symmetric Hall current. (d) A quasiparticle comprising a real electron (blue) and an image charge (gray) with the same spin. (e) Dynamics of an electron and its image in the incompressible strip, depicting skipping and cycloid-type motions. The quasiparticle has spin $S = 1$. The down spin implies that the g factor is negative (17). (f) Skipping motion of two correlated quasiparticles forming total spin $S = 2$.

It will be clarified below that the formation of an $S = 1$ quasiparticle yields three split states and the major plateaus at filling factors $p/3$, where p denotes positive integers not larger than the denominator, and the formation of two correlated quasiparticles of total spin $S = 2$ yields five split states and the second major set of plateaus at $\nu = p/5$. Plateaus at $\nu = p/7$ appear in the next stage by three correlated quasiparticles of total spin $S = 3$. All odd-denominator filling factors existing in the region $\nu \leq 1$ appear as the splitting hierarchy continues down. Such hierarchical separation has been proposed without specific dynamics (18).

To fully understood the FQHE from a fundamental point of view, one must explain the Hall resistivity curve (7) in connection with the quasiparticle energy gaps (19) while remaining consistent with the Hall current profile (16) we discussed above. Therefore, these three essential experiments must be studied within a single theoretical framework.

For this purpose, we construct a Hamiltonian based on the above discussions on electron motion in an incompressible strip. A primitive Hamiltonian of a quantum Hall system is composed of a term giving the LLs, a Zeeman term for individual electrons, electrostatic interactions giving the incompressible strips, and inter-electron interaction in a two-dimensional layer. The latter two are rewritten as a term describing quasiparticle correlations discussed above, which is represented by the sum of the Zeeman terms for correlated quasiparticles. Thus, the Hamiltonian is written as

$$H = \frac{\sum_i (\vec{p}_i + e\vec{A}_i)^2}{2m_0} - \sum_i g^* \mu_B \frac{\vec{s}_i}{\hbar}\cdot\vec{B} - \sum_{n=1}^{\infty} (g^{cb}\mu_B^{cb})_n \frac{\vec{S}_n}{\hbar}\cdot\vec{B}, \tag{1}$$

where m_0 is bare electron mass, $\vec{p}$ and $\vec{A}$ are electron momentum and vector potential, respectively, g^* is the effective Landé g factor in the Hall bar (17), $\mu_B = e\hbar/2m_0$ is the Bohr magneton where $\hbar = h/2\pi$ with Planck constant h, $\vec{s}_i$ is the spin operator of an electron, and $\vec{S}_n$ denotes total spin operator of correlated n quasiparticles. The coefficients $(g^{cb}\mu_B^{cb})_n$, which are written analogously to the previous term, are filling-dependent free parameters.

The Hamiltonian in Eq. (1) is easily diagonalizable by setting $\vec{B} = B\hat{z}$, which gives $S_n^z|\chi\rangle = j_n\hbar|\chi\rangle$, where $j_n = -n, \cdots, 0, \cdots, n$ for integral spin value $S_n = n$. Even though we consider an FQH system with fully polarized electrons occupying the LLL (20), all possible values of j_n are allowed because of level mixing (21) between the up and down spin levels. Thus, the energy eigenvalues for a given filling factor ν are given by

$$E^{\nu}_{N,\sigma,j_n} = \hbar\omega_c(N + 1/2 - \zeta\sigma - \sum_n \delta_{n,\nu} j_n), \tag{2}$$

where $\omega_c = eB/m_c^*$ with m_c^* the cyclotron effective mass, $N = 0$, $\zeta = (g^*/4)(m_c^*/m_0)$, $\sigma = -1$, and $\delta_{n,\nu}$ are free parameters replacing $(g^{cb}\mu_B^{cb})_n$ and representing the degree

of n-particle correlation for a given ν. The free parameters $\delta_{n,\nu}$ are fixed by fitting Hall resistivity and energy gaps simultaneously.

For single quasiparticle dynamics ($n = 1$), three eigenstates are separated by δ_1, and each state has degeneracy $D_L^{(1)} = eB/3h$, implying that a composite boson behaves as if it has a fractional charge of $e/3$ in transport under a Hall bias. Two correlated quasiparticles ($n = 2$) split each state of $n = 1$ into five separated by δ_2, while three correlated quasiparticles ($n = 3$) further separates each state of $n = 2$ into seven by δ_3, as shown in Fig. 2. In the limit $n \to \infty$, one can identify that the half-filling state ($\nu = 1/2$) is gapless.

FQH resistivity can be attained by considering classical Hall resistivity, $\rho_{xy} = B/e\rho_c$, in a quantum mechanical manner. Carrier density ρ_c is the density of electrons in the incompressible regions, and it is given by counting the quantum states determined by j_n below the chemical potential. Since both chemical potential and energy eigenvalues depend on filling factor ν, Hall resistivity ρ_{xy} must be obtained separately for each plateau region by performing a state sum for the Fermi distribution function, i.e. $\rho_{xy}^{\nu} = (B/e)[\sum_k f^{\nu}(E_k)]^{-1}$, where $\sum_k f^{\nu}(E_k) = (eB/h)\sum_{\{j_n\}}[1 + \exp\{(E^{\nu}_{0,\sigma=-1,j_n} - \mu^{\nu})/k_BT\}]^{-1}$ for the LLL and $\sum_{\{j_n\}}$ means $\frac{1}{3\cdot5\cdot7\cdots}\sum_{j_1=-1}^{+1}\sum_{j_2=-2}^{+2}\sum_{j_3=-3}^{+3}\cdots$ (18).

In Fig. 3, we plot our theoretical Hall resistivity for $\nu \leq 1$ superimposed on the experimental data (7). In obtaining Fig. 3, we use $m_c^*/m_0 = 0.067$ of GaAs and $g^* = -0.18$ (17), which give $\hbar\omega_c = (1.73\text{meV/T})B$ and $\zeta = -0.003$, respectively. We calculate at temperature $T = 10$ mK using the values of $\delta_{n,\nu}$ given in Table I and chemical potentials given in the inset of Fig. 3. Hall resistivity and chemical potential are matched by the same colors. Chemical potential controls the horizontal position of the resistivity curve. Agreement with the experimental data (gray) is nearly perfect.

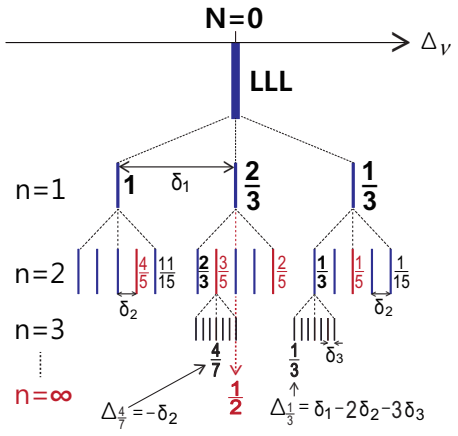

FIG. 2: Level splitting by multi-particle correlations. Dimensionless part of quasiparticle energy Δ_ν is given by the degrees of n-particle correlation $\delta_{n,\nu}$. Examples are given for $\Delta_{1/3}$ and $\Delta_{4/7}$ considering up to $n = 3$. The gapless nature of half-filling state is clarified in the limit of the splitting hierarchy.

One interesting aspect of Fig. 3 is the Fermi liquid feature (22) of the orange section around $\nu = 1/2$, which is a part of the gray dashed line. This feature is consistent with the zero-gap state of $\nu = 1/2$ shown in Fig. 2. Then, considering the half-filling state as the Fermi level classifies the odd-denominator filling factors as follows: the sequences $\nu = q/(2q+1)$, $\nu = q/(2q+3)$, $\nu = q/(2q+5)$, $\cdots$, where $q = 1, 2, \cdots$, belong to particle states, while corresponding hole states are $\nu = 1 - q/(2q+1)$, $\nu = 1-q/(2q+3)$, $\nu = 1-q/(2q+5)$, $\cdots$, respectively. These particle and hole sequences cover all odd-denominator filling factors observed in the region $\nu < 1$ (23).

Finally, we obtain the quasiparticle energy gap, which is defined by the energy at plateau state ν from the Fermi level $\nu = 1/2$. Since Δ_ν shown in Fig. 2 denotes the dimensionless part of energy gap, we need the energy scale part $\hbar eB_{\text{eff}}/m_{cb}^*$ analogous to $\hbar eB/m_c^*$, where $B_{\text{eff}}^{\nu} = |B_\nu - B_{1/2}|$ and m_{cb}^* denotes the cyclotron effective mass of a composite boson. Therefore, we write the quasiparticle energy gap as $E_\nu^G = (\hbar eB_{\text{eff}}^{\nu}/m_{cb}^*)|\Delta_\nu|$. In Fig. 4, we plot E_ν^G using the values given in Table I and $m_{cb}^*/m_0 = 0.21$. Note that Δ_ν in Table I are given in terms of the degree of n-particle correlation, $\delta_{n,\nu}$, which determine the Hall resistivity curve in Fig. 3. The experimental data (black squares) (19) are superimposed for comparison, and the agreement is perfect. The red crosses at $\nu = 5/7$ and $4/5$, which deviate from the straight line, belong to the hole-state sequence $\nu = 1-q/(2q+3)$. We neglect the effect of δ_4 in obtaining energy gaps.

Our understanding of Fig. 4 is somewhat different from the previous explanation (6, 19, 24). We believe that a gapless region may indeed exist, and that it covers the region indicated by the red bar or orange area ranging out to the two points where the straight lines meet the

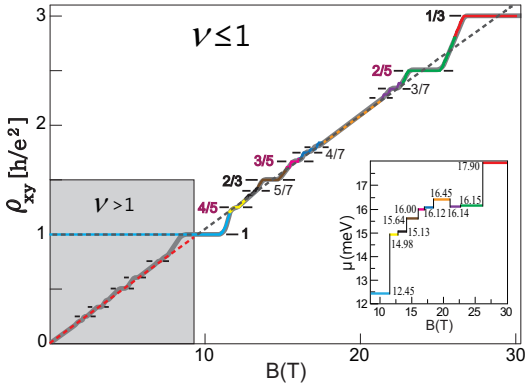

FIG. 3: Theoretical Hall resistivity superimposed on the experimental data (7). The gray dashed line represents the full resistivity line for $\nu = 1/2$, and the red dashed line is an extension of the gray. The chemical potentials in the inset are matched to the Hall resistivity line according to color.

TABLE I: **Values of $\delta_{n,\nu}$, dimensionless part Δ_ν, and $B_{\rm eff}$(T).**

Color	Red	Green	Violet	Orange	Blue	Magenta	Brown	Black	Yellow	Cyan
ν	1/3	2/5	3/7	1/2	4/7	3/5	2/3	5/7	4/5	1
δ_1	0.296	0.30	0.305	0.335	0.302	0.28	0.28	0.253	0.253	0.123
$\delta_2 \times 10$	0.48	0.82	0.99	0.67	1.21	1.0	1.0	0.48	0.57	0.11
$\delta_3 \times 10^2$	0.35	0.29	1.86	0.96	4.6	2.0	0.5	0.57	0.57	0.45
$\delta_4 \times 10^3$	0.3	0.3	0.3	1.0	0.3	0.3	0.3	0.3	0.3	0.3
Δ_ν	†	$2\delta_2$ $-3\delta_3$	δ_2 $+\delta_3$		$-\delta_2$	$-\delta_2$ $-3\delta_3$	$-2\delta_2$ $-3\delta_3$	‡	¶	
$B_{\rm eff}$(T)	9.5	4.75	3.12		2.43	3.29	4.9	5.7	7.0	

†$\delta_1 - 2\delta_2 - 3\delta_3$; ‡ $-\delta_1 + 2\delta_2 - \delta_3$; ¶ $-\delta_1 + \delta_2 - 3\delta_3$.

zero gap line. More experimental data on energy gaps are needed to study the different classes of filling factor sequences.

In conclusion, we have revealed that both plateau widths and energy gaps are determined by the degree of multi-particle correlations as induced by many-body interaction. Such many-body correlations producing the fine structure of the LLL (Fig. 2) are responsible for the essential features of the FQHE. We proved this fact by reproducing experimental Hall resistivity and energy gaps for $\nu \leq 1$. This study is restricted to the LLL because the region $\nu > 1$ contains the problems of spin polarization (20) and even-denominator filling $\nu = 5/2$ that is still under debate. We will study the challenging $\nu > 1$ region separately as our next subject for understanding the FQHE.

The author appreciates T. Toyoda, J. Weis, R. Haug, and A. Gauss for their valuable discussions and help. This work was supported by Project Code (2017R1D1A1A02017587) and partially supported by a KIAS grant funded by the MSIP.

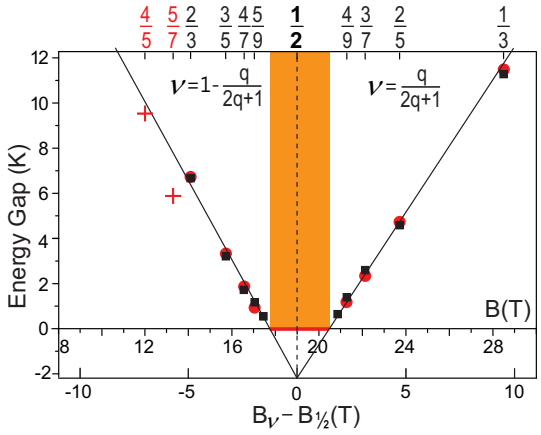

FIG. 4: Quasiparticle energy gaps. Theoretical values (red circles) are obtained via $E_\nu^G = (0.671\text{K/T})(m_0/m_{cb}^*)2|\Delta_\nu| \cdot |B_\nu - B_{1/2}|$ with $m_{cb}^*/m_0 = 0.21$. They are superimposed on experimental data (black squares) (19). Filling factors are located on the upper horizontal axis. The data for $\nu = 4/9$ and 5/9 are obtained using the relations $\Delta_{4/9} = \delta_2 - \delta_3 - \delta_4$ and $\Delta_{5/9} = -\delta_2 + \delta_3 + 2\delta_4$, and using δ_n values for $\nu = 3/7$ and 4/7 in Table I, respectively. Filling factors $\nu = 4/5$ and 5/7 (red crosses) belong to the hole-state sequence $\nu = 1 - q/(2q+3)$.

[1] K. von Klitzing, G. Dorda, M. Pepper, New Method for High-accuracy Determination of the Fine-structure Constant Based on Quantized Hall Resistance. *Phys. Rev. Lett.* **45**, 494-497 (1980).

[2] D. C. Tsui, H. L. Stormer, A. C. Gossard, Two-dimensional Magnetotransport in the Extreme Quantum Limit. *Phys. Rev. Lett.* **48**, 1559-1562 (1982).

[3] J. G. Bednorz, K. A. Müller, Possible high Tc superconductivity in the BaLaCuO system. *Zeit. für Phys. B* **64 (2)**, 189-193 (1986).

[4] R. B. Laughlin, Anomalous Quantum Hall Effect: an Incompressible Quantum Fluid with Fractionally Charged Excitations. *Phys. Rev. Lett.* **50**, 1395-1398 (1983).

[5] J. K. Jain, Composite-Fermion Approach to the Fractional Quantum Hall Effect. *Phys. Rev. Lett.* **63**, 199-202 (1989).

[6] J. K. Jain, *Composite Fermions* (Cambridge Univ. Press, Cambridge, 2007).

[7] J. P. Eisenstein, H. L. Stormer, The Fractional Quantum Hall Effect. *Science* **248**, 1510-1516 (1990).

[8] B. I. Halperin, Quantized Hall conductance, current-carrying edge states, and the existence of extended states in a two-dimensional disordered potential. *Phys. Rev. B* **25**, 2185-2190 (1982).

[9] R. J. Haug, Edge-state transport and its experimental consequences in high magnetic fields. *Semicond. Sci. Technol.* **8**, 131-153 (1993).

[10] M. Büttiker, Absence of backscattering in the quantum Hall effect in multiprobe conductors. *Phys. Rev. B* **38**, 9375-9389 (1988).

[11] K. Lai *et al.*, Imaging of Coulomb-Driven Quantum Hall Edge States. *Phys. Rev. Lett.* **107**, 176809 (2011).

[12] H. Ito *et al.*, Near-Field Optical Mapping of Quantum Hall Edge States. *Phys. Rev. Lett.* **107**, 256803 (2011).

[13] M. E. Suddards, A. Baumgartner, M. Henini, C. J. Mellor, Scanning capacitance imaging of compressible and incompressible quantum Hall effect edge strips. *New J. Phys.* **14**, 083015 (2012).

[14] D. B. Chklovskii, B. I. Shklovskii, L. I. Glazman, Electrostatics of edge channels. *Phys. Rev. B* **46**, 4026-4034 (1992).

[15] K. Lier, R. R. Gerhardts, Self-consistent calculations of edge channels in laterally confined two-dimensional electron systems. *Phys. Rev. B* **50**, 7757-7767 (1994).

[16] A. Gauss *A Scanning Single-Electron Transistor Array Microscope Probes the Hall Potential Profile in the Fractional Quantum Hall Regime* (PhD thesis, University of Stuttgart, 2019).

[17] M. J. Snelling *et al.*, Magnetic g factor of electrons in $GaAs/Al_xGa_{1-x}As$ quantum wells. *Phys. Rev. B*, **44**, 11345-11352 (1991).

[18] T. Toyoda, Magnetic induction dependence of Hall resistance in Fractional Quantum Hall Effect. *Sci. Rept.* **8**, 12741 (2018).

[19] R. R. Du, H. L. Stormer, D. C. Tsui, L. N. Pfeiffer, K. W. West, Experimental evidence for new particles in the fractional quantum Hall effect. *Phys. Rev. Lett.* **70**, 2944-2947 (1993).

[20] I. V. Kukushkin, K. v. Klitzing, K. Eberl, Spin Polarization of Composite Fermions: Measurements of the Fermi Energy. *Phys. Rev. Lett.* **82**, 3665-3668 (1999).

[21] I. Sodemann, A. H. MacDonald, Landau level mixing and the fractional quantum Hall effect. *Phys. Rev. B* **87**, 245425 (2013).

[22] B. I. Halperin, P. A. Lee, N. Read, Theory of the half-filled Landau level. *Phys. Rev. B* **47**, 7312-7343 (1993).

[23] W. Pan *et al.*, Experimental studies of the fractional quantum Hall effect in the first excited Landau level. *Phys. Rev. B* **77**, 075307 (2008).

[24] H. L. Stormer, D. C. Tsui, A. C. Gossard, The fractional quantum Hall Effect. *Rev. Mod. Phys.* **71**, S298-S305 (1999).